Osteoarthritis and Cartilage 21 (2013) 505–513

Osteoarthritis and Cartilage

OARSI OSTEOARTHRITIS RESEARCH SOCIETY INTERNATIONAL

Cell deformation behavior in mechanically loaded rabbit articular cartilage 4 weeks after anterior cruciate ligament transection

S.M. Turunen †*, S.-K. Han ‡§‖, W. Herzog ‡§, R.K. Korhonen †

† *Department of Applied Physics, University of Eastern Finland, POB 1627, FI-70211 Kuopio, Finland*
‡ *Human Performance Laboratory, Faculty of Kinesiology, University of Calgary, Calgary, AB, Canada*
§ *Mechanical & Manufacturing Engineering, Schulich School of Engineering, University of Calgary, Calgary, AB, Canada*
‖ *Fischell Department of Bioengineering, University of Maryland, MD, USA*

ARTICLE INFO

Article history:
Received 2 April 2012
Accepted 7 December 2012

Keywords:
Articular cartilage
Chondrocytes
Mechanics
Fluorescence microscopy
Osteoarthritis
ACLT rabbit model

SUMMARY

Objective: Chondrocyte stresses and strains in articular cartilage are known to modulate tissue mechanobiology. Cell deformation behavior in cartilage under mechanical loading is not known at the earliest stages of osteoarthritis. Thus, the aim of this study was to investigate the effect of mechanical loading on volume and morphology of chondrocytes in the superficial tissue of osteoarthritic cartilage obtained from anterior cruciate ligament transected (ACLT) rabbit knee joints, 4 weeks after intervention.

Methods: A unique custom-made microscopy indentation system with dual-photon microscope was used to apply controlled 2 MPa force-relaxation loading on patellar cartilage surfaces. Volume and morphology of chondrocytes were analyzed before and after loading. Also global and local tissue strains were calculated. Collagen content, collagen orientation and proteoglycan content were quantified with Fourier transform infrared microspectroscopy, polarized light microscopy and digital densitometry, respectively.

Results: Following the mechanical loading, the volume of chondrocytes in the superficial tissue increased significantly in ACLT cartilage by 24% (95% confidence interval (CI) 17.2–31.5, $P < 0.001$), while it reduced significantly in contralateral group tissue by −5.3% (95% CI −8.1 to −2.5, $P = 0.003$). Collagen content in ACLT and contralateral cartilage were similar. PG content was reduced and collagen orientation angle was increased in the superficial tissue of ACLT cartilage compared to the contralateral cartilage.

Conclusions: We found the novel result that chondrocyte deformation behavior in the superficial tissue of rabbit articular cartilage is altered already at 4 weeks after ACLT, likely because of changes in collagen fibril orientation and a reduction in PG content.

Introduction

Chondrocytes are responsible for producing articular cartilage matrix molecules, proteoglycans (PGs) and collagen, and for maintaining the integrity of the extracellular matrix (ECM)[1]. Interstitial fluid is also an important component of the ECM[1–3]. Chondrocyte volume and morphology are known to change both under mechanical stress[4–9] and during the progression of osteoarthritis (OA)[10]. Altered cell biomechanics could lead to changes in cell biosynthesis during OA[8,9], however, cell responses to mechanical loading at the very early stages of OA onset are not known *in vivo* or *in situ*.

First signs of OA, usually seen in the superficial cartilage, include cartilage hydration and swelling[1,11–13], alterations in the collagen network[14], fibrillation of the cartilage surface, and reduced PG content[1,11–15]. Later in the disease, fibrillation of the cartilage surface reaches deeper zones and eburnation of the subchondral bone can be detected[14]. Although OA, and associated cartilage degeneration, have been studied extensively, the very onset of the disease, and the changes in the cell mechanics as well as the relation between cell responses and structural changes of the tissue, remain virtually unknown.

Animal models are widely used to study the progression of OA using mechanical interventions, such as meniscectomy[16,17], ligament transection[18–22] or a combination of the two[23,24]. These procedures lead to changes in joint loading and kinematics which, in turn, lead to the onset and progression of OA[20,25]. Anterior

* Address correspondence and reprint requests to: S.M. Turunen, Department of Applied Physics, University of Eastern Finland, POB 1627, FI-70211 Kuopio, Finland. Tel: 358-40-355-2512; Fax: 358-17-163266.
E-mail addresses: siru.turunen@uef.fi (S.M. Turunen), sangkuy.han@hotmail.com (S.-K. Han), walter@kin.ucalgary.ca (W. Herzog), rami.korhonen@uef.fi (R.K. Korhonen).

1063-4584/$ – see front matter © 2012 Osteoarthritis Research Society International. Published by Elsevier Ltd. All rights reserved.
http://dx.doi.org/10.1016/j.joca.2012.12.001

cruciate ligament transection (ACLT) in rabbits is a commonly used model that has been shown to mimic human OA structurally, biologically and biochemically[26–29]. It has been found that degenerative changes in the rabbit ACLT model may occur as early as 4–12 weeks after intervention[26,30–32]. For example, Hashimoto *et al.*[32] detected osteophyte formation at 4 weeks following ACLT in rabbit femoral condyles. Also, Yoshioka *et al.*[26] found fibrillation of the femoral articulating surfaces, and thickening of the cartilage 4 weeks following ACLT. At 8 weeks after ACLT, moderate/severe OA was already present[26]. Finally, Papaioannou *et al.*[30] found fissures in cartilage at different locations of the rabbit knee at 8 weeks after ACLT.

Although changes in cartilage tissue during OA have been studied extensively, there is little information on the corresponding responses of chondrocytes. Han *et al.*[33] developed a confocal microscopy indentation system for studying *in situ* chondrocyte mechanics. This system allows chondrocytes to be studied in their native environment without the need to isolate cells from the ECM or to prepare explants, which would affect the mechanical environment and deformation behavior of the cells[34]. Using this system, Han *et al.*[31] discovered that at 9 weeks after ACLT cell volumes increased in mechanically compressed cartilage, while opposite cell volume behavior was detected in contralateral and normal joint cartilage.

The purpose of this study was to determine (1) if cell responses in mechanically compressed articular cartilage are altered as early as 4 weeks after ACLT (very early stage of OA) and (2) if the cell mechanics change before structural alterations in the tissue, or if alterations in cell mechanics are related to detectable structural changes in the ECM. Unilateral ACLT was performed in 10 rabbits, and chondrocyte volume and morphology in the superficial tissue were quantified in fully intact rabbit patellar cartilage in loaded and unloaded states using a custom-made testing system coupled with dual-photon excitation microscope[33]. Depth-wise collagen content, collagen fibril orientation, and PG content were quantified with Fourier transform infrared (FTIR) microspectroscopy, polarized light microscopy (PLM) and digital densitometry (DD), respectively. We concentrated on the superficial cartilage in which the first changes of OA typically occur[11,35,36].

Methods

Animal model

Unilateral ACLT was conducted for 10 skeletally mature female New Zealand white rabbits (*Oryctolagus cuniculus*, age 14 months, weight 5.4 ± 0.6 kg) under general anesthesia. The use of female rabbits only provided us with a homogeneous group. The contralateral side was not subjected to any surgical procedure. Animals were sacrificed 4 weeks after ACLT (29 ± 1 days, this small standard deviation (SD) was due to technical reasons), the knee joints from the experimental and contralateral side were harvested, and the intact patellae were removed from the joints. This procedure was carried out according to the guidelines of the Canadian Council on Animal Care and was approved by the committee on Animal Ethics at the University of Calgary.

Tissue preparation

Specimen preparation was done similarly as described previously[31,33]. Briefly, fluorescein conjugated Dextran (3 kDa molecular weight, excitation 488 nm, emission 500 nm, Invitrogen, Molecular Probes, OR, USA) was used for staining the samples. First, Dextran was suspended in Dulbecco's Modified Eagle's Medium (DMEM, Gibco, OR, USA) with the final concentration of 4.8 mg/ml. The Dextran concentration was higher than previously[31], because the quantum yield was lower. This way similar fluorescent image quality as before was ensured. Then the intact patella was incubated in the solution for 4 h at 4°C. After staining, the samples were washed in phosphate buffered saline (PBS, 300–304 mOsm, pH 7.4) two times for 10 min in order to remove excess Dextran. After washing, the samples were fixed in a custom-made sample holder with dental cement and a self-tapping bone screw in 15–30 min (Fine Science Tools, North Vancouver, BC, Canada). During and after fixation, the samples were kept moist with PBS.

Mechanical indentation and microscopy

Mechanical indentation of the cartilage samples was done according to a previously described protocol[31] using a unique microscopy indentation system described in detail earlier [Fig. 1(a)][33]. Briefly, a light transmissible indentation system (round glass indenter, total diameter 2 mm) mounted on the stage of a dual-photon microscope (Chameleon XR infrared laser, Coherent Inc., USA) directly in front of the objective (40× 0.8 NA water-immersion objective, Zeiss Inc., Germany) was used for capturing images of chondrocytes. First, a small preload (0.1–0.2 MPa) was applied in order to ensure a contact between the indenter and the sample. A pressure of 2 MPa was then applied on the middle of the patellar sample (corresponding to submaximal compression load[37]) at an average speed of 10 μm/s. After reaching the wanted stress level, the displacement was held constant for 20 min, thus the stress level was reduced to 0.71 MPa (95% confidence interval (CI) 0.61–0.81 MPa) and 0.78 MPa (95% CI 0.64–0.92 MPa) in ACLT and contralateral samples ($P = 0.427$), respectively, in the end of the experiment[38]. Image stacks (*xy* plane, 512 × 512 pixels, pixel size 0.41 μm × 0.41 μm) were obtained with 0.5 μm vertical *z*-axis increments up to 60 μm in depth from the cartilage surface (same parameters as in[31,33,39,40]), while the analyzed cells were located approximately at 20 μm depth. The system was calibrated by measuring polystyrene microspheres (Polysciences Inc., Warrington, PA, USA) of 5.93 ± 0.05 μm in diameter in Dextran stained agarose gel using the same setup as in the actual cell measurement tests. A correction factor for *z*-axis distortion was obtained by dividing the known microsphere diameter with their apparent height[31,33].

The acquired images were imported into image analysis software ImageJ (National Institute of Health, USA), and the morphology of approximately 10 superficial tissue cells from each sample (image stack) was analyzed before and after loading, i.e., individual cells were tracked ($n = 8$ samples, $N = 77–79$/group). The number of samples used for cell morphometric analysis and local tissue strains was eight, since the Dextran labeling of the ECM did not work properly for the first two specimens. Bright fluorescence of the ECM was detected still after loading (at most 10–15% reduction in the fluorescence intensity), ensuring minimal photobleaching. Image thresholds were defined from intensity histograms individually for each cell with its background using the median value[33]. The Visualization Toolkit 5.2.0 (Kitware Inc., USA) was used for reconstructing 3D-images of the cells, and a code, programmed with Python, was used for calculating cell volumes (for more details see[41]). Briefly, a Gaussian convolution of the original images was performed for the analysis of cell volumes. Iso-surfaces of the cell volumes were then created, followed by forming triangle polygons representing the iso-surfaces. Finally, cell volumes were calculated from the triangle meshes. Width and depth (*x*- and *y*-directions) of cells were defined along the minor and major axes of the cell cross sections taken perpendicular to the height of the cells (*z*-direction) using Matlab R2007b (MathWorks Inc., USA)[31,33].

The local axial ECM strain was defined by measuring the change in distance between the centroids of paired cells in the unloaded and loaded configuration in axial direction ($n = 8$). The local

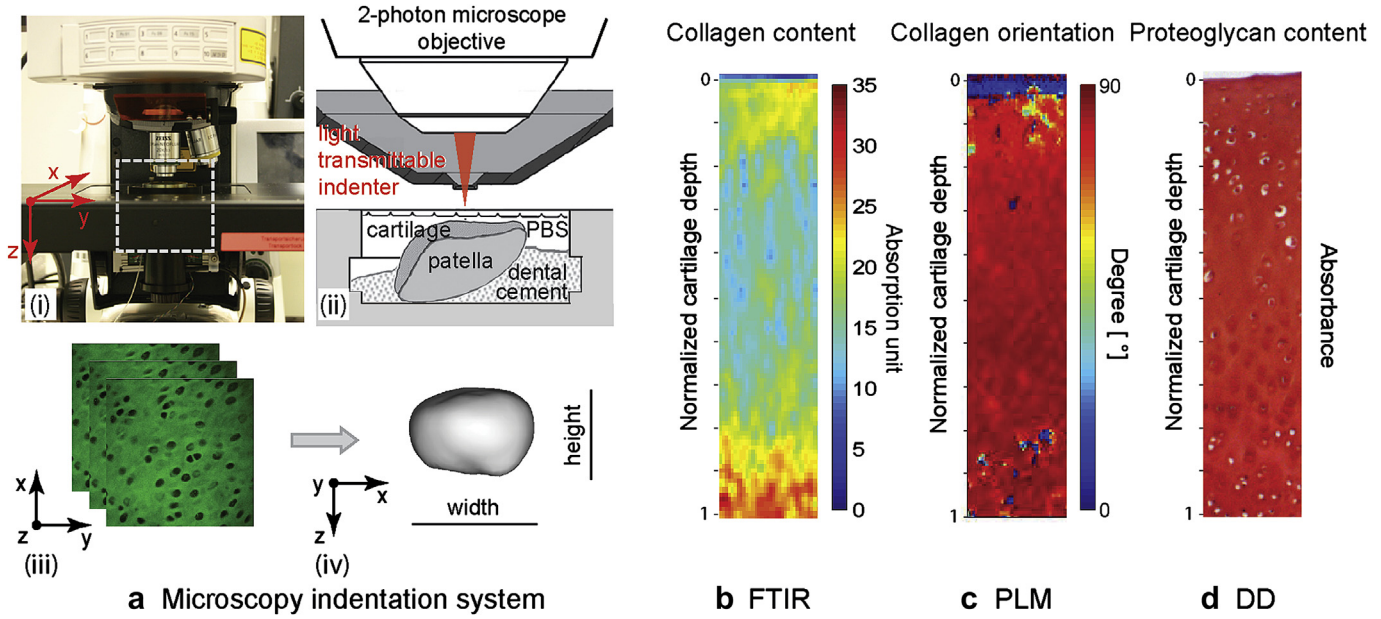

Fig. 1. (a) (i) Mechanical indentation system mounted on a dual-photon microscope, (ii) a schematic presentation of the measurement setup[33], (iii) typical microscopic images of the Dextran stained samples, (iv) a 3D-presentation of a chondrocyte, and representative FTIR (b), PLM (c) and DD (d) images for determination of collagen content, collagen orientation and PG content, respectively.

transversal ECM strain was defined by selecting four easily detectable cells in the same focal plane (x–y) of the dual-photon microscopic images and by analyzing the change in the distance between the cells in the unloaded and loaded configuration ($n = 8$)[7,31]. The global tissue strain was calculated by dividing the tissue axial compression by the total cartilage thickness ($n = 10$). The Young's modulus of the samples was calculated using the equation by Hayes *et al.*[42] ($n = 10$):

$$E = E_{\text{measured}}\left(\frac{\pi a}{2h\kappa}\left(1-\nu^2\right)\right),$$

where E_{measured} is the modulus calculated directly from the experiments at equilibrium (stress divided by strain), a is the radius of the indenter, h is the thickness of the cartilage, ν is the Poisson's ratio (estimated to be 0.16[43]) and κ is the novel scaling factor[44]. Matlab R2007b was used for these analyses.

Microscopic and spectroscopic analysis of tissue structure

Sample processing

Following indentation testing, patellae were fixed in formalin, decalcified with ethylenediaminetetraacetic (EDTA), dehydrated, and treated with xylene before embedding in paraffin ($n = 10$) (for details see[45–47]). Microscopic sections [three slices per sample, mid-region of the patella, i.e., the same area where the cell loading occurred, Fig. 1(a)] were cut perpendicular to the cartilage surface. For FTIR microspectroscopy and PLM five μm thick sections were deparaffinized and PGs were removed with hyaluronidase digestion (1000 U/ml hyaluronidase, Sigma–Aldrich, St. Louis, MO, USA). For DD, the samples were three μm thick and stained with safranin O. Sections for FTIR were placed on ZnSe windows, while those for PLM and DD were placed on standard microscopic slides.

Structural analysis

The spatial collagen content was determined with FTIR microspectroscopy ($n = 10$). Molecular components in biological samples have a characteristic infrared absorption spectrum, thus, the distribution of the components can be quantified [Fig. 1(b)][48–50]. Depth-dependent collagen fibril orientation was analyzed using PLM [Fig. 1(c), $n = 10$]. The orientation of the collagen fibrils leads to an optical path difference (birefringence) of the light[47,51,52]. The measured birefringence depends on the angle between the axis of the polarization and fibril, and thus, collagen orientation can be measured. Spatial PG content was determined by quantifying the optical density (OD) of safranin O stained sections using DD [Fig. 1(d), $n = 10$]. Safranin O is a cationic dye which binds to negatively charged glycosaminoglycans. OD values have been found to correlate with the PG concentrations in cartilage tissue[53]. See Supplementary material for more details.

Statistical analysis

All results are shown as mean and 95% CI. The number of samples is given as "n" and number of cells as "N". When comparing cell parameters between groups (ACLT, contralateral), a one-way analysis of variance (ANOVA) was applied for individual cells (N). The structural and compositional differences between the samples (n) were evaluated with Wilcoxon signed rank test. The level of significance was 0.05 for all of the tests. All statistical analyses were performed with SPSS 17.0 (SPSS Inc, Chicago, IL, USA).

Results

Mechanical indentation tests

Before loading, chondrocyte volumes in ACLT patellae were significantly smaller than in contralateral patellae [Table I, Fig. 2(a)]. Similarly, cell height, width and depth in the ACLT group were significantly smaller compared to the contralateral group [Table I, Fig. 2(b–d)]. Cell aspect ratios in the ACLT and contralateral joint cartilage before the mechanical loading were similar: height/width: 0.47 (95% CI 0.45–0.50) and 0.47 (95% CI 0.43–0.50) ($P = 0.928$), height/depth: 0.68 (95% CI 0.65–0.71) and 0.66 (95% CI 0.62–0.70) ($P = 0.718$), respectively.

Table I
Cell volume, height, width and depth before loading in ACLT and contralateral groups ($n = 8$), and statistical differences between the groups (P-values)

	ACLT mean (95% CI) ($N = 79$)	CNTRL mean (95% CI) ($N = 77$)	ACLT vs CNTRL P-value
Volume (μm^3)	305 (289–321)	431 (409–453)	<0.001
Height (μm)	5.7 (5.5–5.9)	6.5 (6.2–6.8)	<0.001
Width (μm)	12.6 (12.1–13.0)	14.0 (13.5–14.5)	<0.001
Depth (μm)	8.5 (8.3–8.8)	9.6 (9.4–9.9)	<0.001

Table II
Cell volume, height, width and depth after loading in ACLT and contralateral groups ($n = 8$), and statistical differences between the groups (P-values)

	ACLT mean (95% CI) ($N = 79$)	CNTRL mean (95% CI) ($N = 77$)	ACLT vs CNTRL P-value
Volume (μm^3)	368 (349–387)	405 (384–425)	0.013
Height (μm)	4.7 (4.5–4.8)	4.9 (4.7–5.1)	0.080
Width (μm)	14.8 (14.3–15.3)	15.7 (15.2–16.3)	0.018
Depth (μm)	10.8 (10.5–11.0)	10.9 (10.5–11.2)	0.882

As a result of 2 MPa loading on cartilage surface, volume of the cells increased significantly in the ACLT group, while it decreased significantly in the contralateral patella [Tables II and III, Fig. 2(a)]. Consequently, the average change in cell volume caused by mechanical loading was significantly different in the ACLT compared to the contralateral group [Tables II and III, Fig. 2(a)]. Cell height decreased, while width and depth increased significantly after loading in both groups [Tables II and III, Fig. 2(b–d)]. However, changes in cell width and depth were significantly larger in the ACLT than in the contralateral group, while the change in cell height was significantly larger in the contralateral group [Tables II and III, Fig. 2(b–d)].

The average local axial and transversal ECM strains due to indentation were greater in the ACLT group cartilage compared to the contralateral joint cartilage, but there were no statistically significant difference between the groups ($P = 0.059$ and 0.355, respectively, Fig. 3). Also, the average global tissue strain due to mechanical indentation was greater in the ACLT compared to the contralateral joint cartilage, but this difference was not statistically significant ($P = 0.168$, Fig. 3). The Young's modulus of the ACLT joint cartilage was lower than that of the contralateral joint cartilage (1.8 MPa (95% CI 1.2–2.3 MPa) and 2.4 MPa (95% CI 1.5–3.2 MPa), respectively), but the difference was not statistically significant ($P = 0.162$).

Structural analysis

The average thicknesses of the ACLT and contralateral joint cartilages, 700 μm (95% CI 634–765 μm) and 774 μm (95% CI 709–839 μm), respectively, were not significantly different ($P = 0.106$). Collagen content in the ACLT and contralateral groups was the same throughout the tissue depth ($P > 0.05$) [Fig. 4(a)]. Collagen orientation angle increased significantly in the ACLT group compared to the contralateral group (0–9% of tissue depth, $P < 0.05$) [Fig. 4(b)]. PG content was significantly lower in the ACLT than in the contralateral group tissue [0–24% of tissue depth, $P < 0.05$, Fig. 4(c)].

Discussion

Chondrocyte response to mechanical loading in a very early stage of OA was studied with a rabbit ACLT model 4 weeks after intervention. A mechanical indentation device coupled with a dual-photon microscope was used for studying cell volume and morphology in the superficial tissue before and after mechanical loading. Collagen content, collagen orientation angle and PG content were studied with FTIR microspectroscopy, PLM and DD, respectively, in order to reveal changes in cartilage structure and

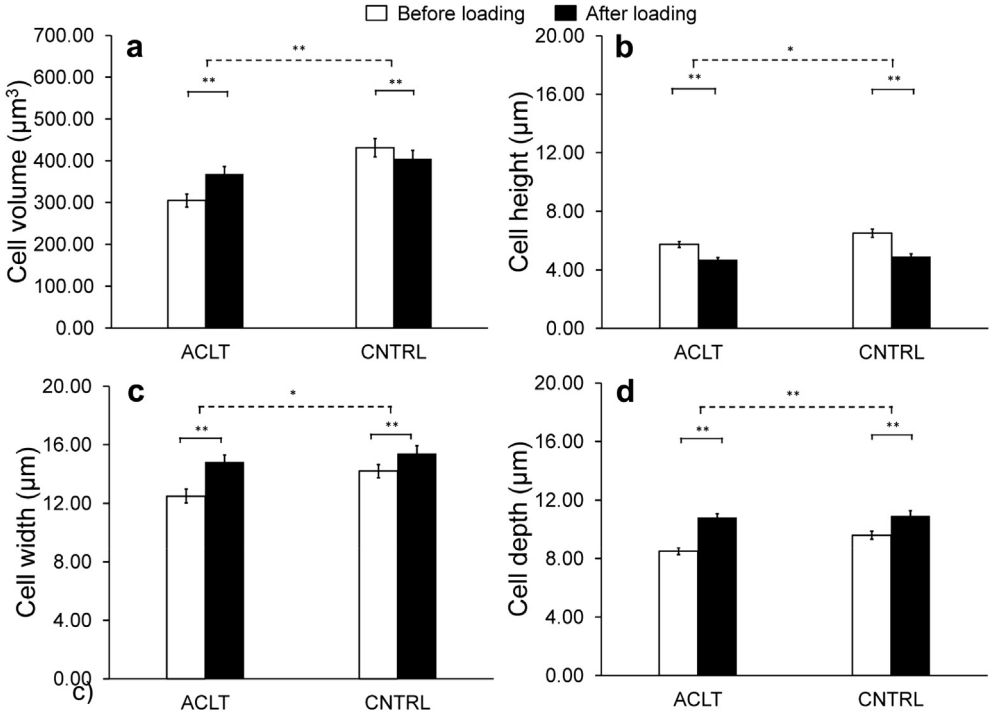

Fig. 2. Cell volume (a), height (b), width (c) and depth (d) in ACLT ($n = 8$, $N = 79$) and in contralateral joint cartilage ($n = 8$, $N = 76$) before (white bar) and after (black bar) mechanical loading, and statistically significant differences between conditions (before/after loading: solid line) and groups (average change after mechanical loading: dashed line). $^{**}P < 0.001$, $^{*}P < 0.05$.

Table III
Average change in cell volume, height, width and depth in ACLT and contralateral groups ($n = 8$) due to mechanical loading, and statistical differences between the groups (*P*-values)

	ACLT mean (95% CI) ($N = 79$)	CNTRL mean (95% CI) ($N = 77$)	ACLT vs CNTRL *P*-value
Change in volume (%)	24.4 (17.2–31.5)	−5.3 (−8.1 to −2.5)	<0.001
Change in height (%)	−16.8 (−20.3 to −13.2)	−23.5 (−26.1 to −20.9)	0.003
Change in width (%)	18.7 (15.8–21.5)	13.1 (11.1–15.1)	0.001
Change in depth (%)	26.9 (23.5–30.3)	13.1 (10.0–16.3)	<0.001

composition in a very early stage of OA. With mechanical loading of the cartilage, chondrocyte volume increased in the ACL transected joints, while it decreased in contralateral joints. Collagen orientation angle and PG content were altered in the ACLT group compared to the contralateral group, while collagen content was not different between the ACLT and contralateral joint cartilages. These results suggest that cell deformation behavior in mechanically compressed articular cartilage is altered already 4 weeks after ACLT and that this change could be primarily explained by alterations in collagen orientation angle and PG content.

Collagen fibrillation and reduced PG content have commonly been accompanied as one of the earliest changes in OA[14,35,49,54–56]. Consistent with these studies, here the Benninghoff-like collagen fibril architecture[57–61] was altered only in the superficial cartilage. That is, the orientation angle of the collagen fibers was significantly higher in the ACLT joint cartilage compared to the contralateral joint cartilage, indicating collagen fibrillation in the very early stage of OA. Significantly smaller PG content in the ACLT group cartilage compared to the contralateral joint cartilage was also consistent with aforementioned earlier studies.

Collagen content was the same in ACLT and contralateral joint cartilages. In some earlier studies, collagen content had been found to decrease in early OA[23,49], while it remained unaltered in others[24,62], or decreased only in the later stages of the disease[14,56]. Differences in the results might arise from the use of different measuring techniques (FTIR microspectroscopy, immunohistochemistry), different animals (human, rabbit, bovine), different animal models (ACLT, meniscus removal, Hulth-Telhag, natural OA), different measurement sites (patella, femoral condyles) and different age of the experimental animals. However, our results are consistent with earlier FTIR microspectroscopy studies[24,56], in which collagen content was not altered in early OA.

Cell volume has been found to decrease under mechanical load in normal cartilage[4,5,31]. We found the same for the contralateral

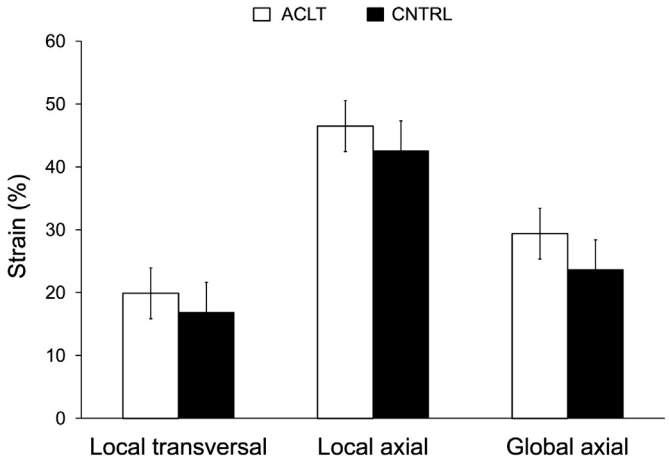

Fig. 3. Local transversal ECM strain ($n = 8$, $N = 21$ pairs), local axial ECM strain ($n = 8$, $N = 72$ pairs) and global axial tissue strain ($n = 10$/group) in ACLT and contralateral joint cartilage. Local strains were defined by comparing the distance between paired cells before and after loading, and global strain by dividing the tissue compression by cartilage thickness (see text for details).

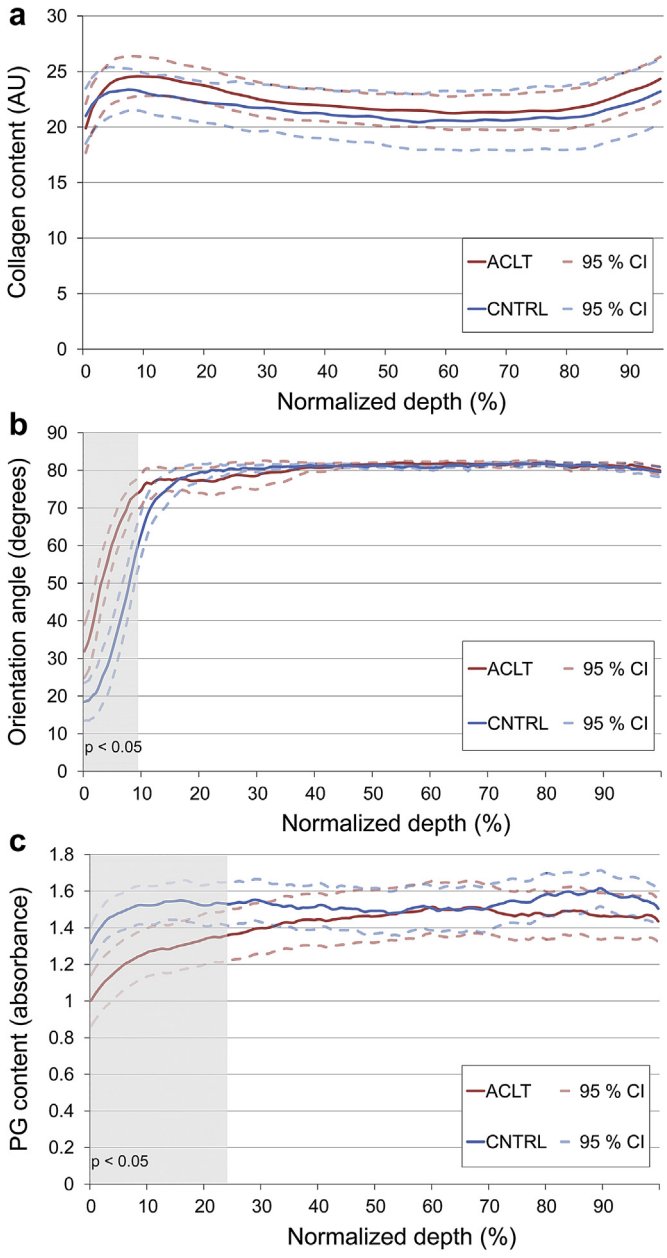

Fig. 4. Collagen content (AU = absorption unit) (a), collagen orientation angle (b) and PG content (c) in ACLT (red line) and contralateral (blue line) groups as a function of tissue depth, defined using FTIR microspectroscopy, PLM and DD, respectively ($n = 10$/group).

joint cartilage. In the ACLT joint cartilage, however, the cell response to mechanical loading was the opposite, and cell volume increased after cartilage loading. The increase in cell volume resulted from large changes in cell width and depth, directions parallel to the cartilage surface. In contrast, chondrocytes were compressed more in the contralateral joint cartilage, while cell expansion in the plane perpendicular to loading was simultaneously smaller, causing reduced cell volume as a result of tissue compression. In agreement with our results, Han *et al.*[31] found an increase in cell volume in OA cartilage (ACLT induced OA, 9 weeks after the intervention), while cell volume decreased in normal cartilage under mechanical load. Also Tanska *et al.*[63] and Korhonen and Herzog[64] found using finite-element modeling that cell volume can increase as a result of cartilage loading.

Even though global and local tissue strains were 10–24% greater and the Young's modulus of the samples was almost 30% smaller in the ACLT group compared the contralateral group, these alterations were not statistically significant. Thus, the explanation for the difference in the behavior of the cells between the groups might not be found in the ECM biomechanics. Broom and Myers[65] saw collagen fiber crimping in the pericellular matrix (PCM) due to mechanical loading, and speculated that this phenomenon could act as a protective mechanism to further loading of normal cartilage. Guilak *et al.*[66] suggested that the PCM acts as a transducer of mechanical load in cartilage, and the deformation from the ECM to cell is shown to be translated non-linearly[67]. Han *et al.*[31] speculated that the PCM amplifies the cell deformations at low strains, and dampens them at large strains. Korhonen and Herzog[64] found that the collagen fibril stiffness of the PCM affects the chondrocyte response to mechanical tissue loading. Most importantly, they found an increase in cell volumes if the fibril stiffness of the PCM decreased sufficiently, as may happen in OA cartilage. This result was confirmed in a recent study[63]. Furthermore, our preliminary findings using finite-element modeling suggest that the amount of fixed charge densities (FCDs) in the PCM contributes to the mechanical response of chondrocytes under tissue compression, and cell volume increases were observed if the FCD was decreased sufficiently (Tanska *et al.* unpublished data). Since we found that the orientation angle of the collagen fibrils was altered and the FCD was reduced significantly in the superficial zone of the ACLT joint cartilage, the protective mechanisms of the PCM and its surroundings in the ECM may have been compromised, resulting in larger cell expansion and increased cell volume following mechanical tissue loading. Unfortunately, our methods were not able to specifically characterize possible minor changes in the PCM. The PCM structure and composition in the very early stage of OA should be characterized with nanoscale techniques, such as transmission electron microscopy. This should give a better indication of the role of the PCM on cell volumetric behavior in OA cartilage under mechanical compression. Microscale finite-element modeling could further clarify the importance of the ECM and PCM properties on chondrocyte deformations in OA cartilage[64,68–72].

The degeneration of cartilage is traditionally estimated with histological grading (e.g., Mankin[73], Osteoarthritis Research Society International (OARSI)[74]). These methods concentrate more on degenerative changes of cartilage throughout the entire tissue depth. In the present study, the applied microscopic and spectroscopic methods provided us with detailed, local characterization of tissue structure and composition[47–52,75]. Specifically for the present study, we wanted to characterize the very first alterations in the superficial tissue. Thus, we think that Mankin or OARSI grading would not have added more detailed information.

In the measurement protocol, we first applied a 2 MPa contact stress, which was followed by a force relaxation for 20 min. The protocol was based on a previous study by Han *et al.*[31]. The applied load of 2 MPa represents a submaximal compression load on the patello-femoral joint[37]. On the other hand, our analysis of cell volume was conducted at 20 min after tissue compression, which is near steady-state with negligible fluid flow, while the solid matrix components should have more important effect on cells. Our stresses (0.71 and 0.78 MPa) and strains (29 and 24 %) at steady-state should be in the physiological range (e.g., Hosseini *et al.*[76]). Local tissue strains of 47% and 43% observed in the present study were also consistent with a study by Shinagl *et al.*[77] in which a 46% local tissue strain was detected in the superficial cartilage under a 16% total (global) strain. These results indicate inhomogeneous tissue structure and composition. Furthermore, choosing a 2 MPa stress level followed by force relaxation enabled us to compare our results to previous study by Han *et al.*[31] where similar investigations were done 9 weeks after ACLT.

Previously it has been shown that the size of the cells increases with the degree of cartilage degeneration[10] and in early OA[31]. In our study, however, we found that at a very early stage of OA, the resting volume of cells was greater in the contralateral joint cartilage compared to the ACLT joint cartilage. Earlier, in a Hulth–Telhag model of OA in rabbits, degenerative changes were observed also in the contralateral side, and it was speculated that in the first weeks after surgery, the healthy leg was probably used more[23]. Interestingly, Rogart *et al.*[23] also reported that the collagen staining in the contralateral group returned close to the level of the control group 14 weeks after the operation. Thus, there might be some adaptation in the cartilage structure/cell behavior after the initial changes, which might even be concentrated primarily on the cell and its vicinity. On the other hand, since the FCD of PGs creates tissue swelling and presumably also contributes to cell resting volume, it may be that smaller cell volume in the ACLT than contralateral joint cartilage is simply related to the reduced superficial PG content.

We did not have a separate normal control group in this study. However, in a recent study cell volume responses following mechanical loading in cartilage from normal control group animals (15 months old) were similar to those observed here in the contralateral group cartilage[31]. Further processed samples of that study showed that normal and contralateral group cartilages had also similar collagen orientation and PG content in the superficial tissue ([78] and unpublished data by Han *et al.*), parameters that are suggested to alter cell deformation behavior in this study. Thus, the contralateral group might be an appropriate sample for a control group within these time limits (4–9 weeks post surgery).

As indicated above, surprisingly there were no significant differences in global and local tissue strains between the groups. The insignificant difference might turn to significant with larger number of samples. On the other hand, in the very early onset of OA, the change in strain might occur first in the cell level due to possible structural alterations in the PCM, whereas ECM strains might increase at later stages of OA, such as was discovered at 9 weeks after the ACLT[31]. The unaltered collagen content might also have had some role to prevent tissue expansion under loading.

To conclude, this is the first study to reveal that changes in the cartilage structure, primarily increased collagen fibrillation and reduced PG content, are already present in the very early stage of OA, and they are accompanied with changes in cell biomechanics. This is an important finding, as in order to be able to prevent, reverse or cure OA, the early developmental phase of OA should be known in detail. As already a minor collagen fibrillation and reduced PG content resulted in changed chondrocyte deformation behavior, possibly leading to changes in cell biosynthesis and further affecting cartilage structure[8,9], strategies and methods for detecting these alterations and preventing or reversing further OA progression should be found.

Author contributions

ST drafted the article and all authors revised it critically and approved the final version to be published.

Study conception and design: ST, RK, S-KH, WH.

Acquisition of data: ST, S-KH.

Interpretation of data: ST, RK, S-KH, WH.

Statistical analysis: ST, RK.

Ethics approval of research on animals

This study was carried out according to the guidelines of the Canadian Council on Animal Care and was approved by the committee on Animal Ethics at the University of Calgary.

Role of the funding source

Study sponsors did not have any involvement in study design, collection, analysis and interpretation of data, in the writing of the manuscript or in the decision to submit the manuscript for publication.

Competing interest statement

Authors have no competing interests.

Acknowledgments

Financial support from the Academy of Finland (projects 218038 and 140730), Sigrid Juselius Foundation, Finland, National Doctoral Programme of Musculoskeletal Disorders and Biomaterials, Finnish Cultural Foundation (North Savo Regional Fund), AHFMR Team grant on OA, Emil Aaltonen Foundation and European Research Council (ERC, project 281180) is acknowledged. The Killam Foundation, the AIHS Team grant on Osteoarthritis, and the Canada Research Chair Programme are also acknowledged for their support. Authors want also to thank Ms Jaana Mäkitalo for assistance in the measurements and Tim Leonard, University of Calgary, for ACL transection of rabbits.

Supplementary material

Supplementary material related to this article can be found at http://dx.doi.org/10.1016/j.joca.2012.12.001.

References

1. Stockwell RA. Cartilage failure in osteoarthritis: relevance of normal structure and function. A review. Clin Anat 1991;4:161–91.
2. Stockwell RA, Meachim G. The chondrocytes. In: Freeman MAR, Ed. Adult Articular Cartilage. Oxford: Alden Press; 1973:51–99.
3. Mankin HJ, Mow VC, Buckwalter JA, Iannotti JP, Ratcliffe A. Form and function of articular cartilage. In: Sheldon RS, Ed. Orthopaedic Basic Science. American Academy of Orthopaedic Surgeons; 1994:1–44.
4. Buschmann MD, Hunziker EB, Kim YJ, Grodzinsky AJ. Altered aggrecan synthesis correlates with cell and nucleus structure in statically compressed cartilage. J Cell Sci 1996;109:499–508.
5. Guilak F. Compression-induced changes in the shape and volume of the chondrocyte nucleus. J Biomech 1995;28:1529–41.
6. Brandt KD, Radin E. The physiology of articular stress – osteoarthrosis. Hosp Pract 1987;22:103–26.
7. Guilak F, Ratcliffe A, Mow VC. Chondrocyte deformation and local tissue strain in articular cartilage: a confocal microscopy study. J Orthop Res 1995;13:410–21.
8. Wong M, Wuethrich P, Buschmann MD, Eggli P, Hunziker E. Chondrocyte biosynthesis correlates with local tissue strain in statically compressed adult articular cartilage. J Orthop Res 1997;15:189–96.
9. Szafranski JD, Grodzinsky AJ, Burger E, Gaschen V, Hung H-H, Hunziker EB. Chondrocyte mechanotransduction: effects of compression on deformation of intracellular organelles and relevance to cellular biosynthesis. Osteoarthritis Cartilage 2004;12:937–46.
10. Bush PG, Hall AC. The volume and morphology of chondrocytes within non-degenerate and degenerate human articular cartilage. Osteoarthritis Cartilage 2003;11:242–51.
11. McDevitt CA, Muir H. Biochemical changes in the cartilage of the knee in experimental and natural osteoarthritis in the dog. J Bone Joint Surg Br 1976;58:94–101.
12. Maroudas A, Venn M. Chemical composition and swelling of normal and osteoarthrotic femoral head cartilage II. Swelling. Ann Rheum Dis 1977;36:399–406.
13. Grushko G, Schneiderman R, Maroudas A. Some biochemical and biophysical parameters for the study of the pathogenesis of osteoarthritis: a comparison between the processes of ageing and degeneration in human hip cartilage. Connect Tissue Res 1989;19:149–76.
14. Buckwalter JA, Mankin HJ. Articular cartilage II. Degeneration and osteoarthritis, repair, regeneration, and transplantation. J Bone Joint Surg Am 1997;79:612–32.
15. Vignon E. Quantitative histological changes in osteoarthritic hip cartilage. Morphometric analysis of 29 osteoarthritic and 26 normal human femoral heads. Clin Orthop 1974;103:269–78.
16. Young AA, McLennan S, Smith MM, Smith SM, Cake MA, Read RA, *et al*. Proteoglycan 4 downregulation in a sheep meniscectomy model of early osteoarthritis. Arth Res Ther 2006;8:R41.
17. Beveridge JE, Shrive NG, Frank CB. Meniscectomy causes significant in vivo kinematic changes and mechanically induced focal chondral lesions in a sheep model. J Orthop Res 2011;29:1397–405.
18. Brandt KD, Myers SL, Burr D, Albrecht M. Osteoarthritic changes in canine articular cartilage, subchondral bone, and synovium fifty-four months after transection of the anterior cruciate ligament. Arthritis Rheum 1991;34:1560–70.
19. Herzog W, Diet S, Suter E, Mayzus P, Leonard TR, Müller C, *et al*. Material and functional properties of articular cartilage and patellofemoral contact mechanics in an experimental model of osteoarthritis. J Biomech 1998;31:1137–45.
20. Herzog W, Adams ME, Matyas JR, Brooks JG. Hindlimb loading, morphology and biochemistry of articular cartilage in the ACL-deficient cat knee. Osteoarthritis Cartilage 1993;1:243–51.
21. Bray RC, Shrive NG, Frank CB, Chimich DD. The early effects of joint immobilization on medial collateral ligament healing in an ACL-deficient knee: a gross anatomic and biomechanical investigation in the adult rabbit model. J Orthop Res 1992;10:157–66.
22. Williams JM, Felten DL. Effects of surgically induced instability on rat knee articular cartilage. J Anat 1982;134:103–9.
23. Rogart JN, Barrach HJ, Chichester CO. Articular collagen degradation in the Hulth–Telhag model of osteoarthritis. Osteoarthritis Cartilage 1999;7:539–47.
24. Bi X, Yang X, Bostrom MPG, Bartusik D, Ramaswamy S, Fishbein KW, *et al*. Fourier transform infrared imaging and MR microscopy studies detect compositional and structural

changes in cartilage in a rabbit model of osteoarthritis. Anal Bioanal Chem 2007;387:1601–12.
25. Setton LA, Mow VC, Müller FJ, Pita JC, Howell DS. Mechanical properties of canine articular cartilage are significantly altered following transection of the anterior cruciate ligament. J Orthop Res 1994;12:451–63.
26. Yoshioka M, Coutts RD, Amiel D, Hacker SA. Characterization of a model of osteoarthritis in the rabbit knee. Osteoarthritis Cartilage 1996;4:87–98.
27. Sah RL, Yang AS, Chen AC, Hant JJ, Halili RB, Yoshioka M, *et al*. Physical properties of rabbit articular cartilage after transection of the anterior cruciate ligament. J Orthop Res 1997;15: 197–203.
28. Le Graverand M-PH, Eggerer J, Vignon E, Otterness IG, Barclay L, Hart DA. Assessment of specific mRNA levels in cartilage regions in a lapine model of osteoarthritis. J Orthop Res 2002;20:535–44.
29. Vignon E, Bejui J, Mathieu P, Hartmann JD, Ville G, Evreux JC, *et al*. Histological cartilage changes in a rabbit model of osteoarthritis. J Rheumatol 1987;14:104–6.
30. Papaioannou N, Krallis N, Triantafillopoulos IK, Khaldi L, Dontas I, Lyritis GP. Optimal timing of research after anterior cruciate ligament resection in rabbits. Contemp Top Lab Anim Sci 2004;43:22–7.
31. Han S-K, Seerattan R, Herzog W. Mechanical loading of in situ chondrocytes in lapine retropatellar cartilage after anterior cruciate ligament transection. J R Soc Interface 2010;7: 895–903.
32. Hashimoto S, Creighton-Achermann L, Takahashi K, Amiel D, Coutts RD, Lotz M. Development and regulation of osteophyte formation during experimental osteoarthritis. Osteoarthritis Cartilage 2002;10:180–7.
33. Han S-K, Colarusso P, Herzog W. Confocal microscopy indentation system for studying in situ chondrocyte mechanics. Med Eng Phys 2009;31:1038–42.
34. Turunen SM, Lammi MJ, Saarakkala S, Koistinen A, Korhonen RK. Hypotonic challenge modulates cell volumes differently in the superficial zone of intact articular cartilage and cartilage explant. Biomech Model Mechanobiol 2012;11: 665–75.
35. Guilak F, Ratcliffe A, Lane N, Rosenwasser MP, Mow VC. Mechanical and biochemical changes in the superficial zone of articular cartilage in canine experimental osteoarthritis. J Orthop Res 1994;12:474–84.
36. Stockwell RA. Ultrastructural changes in articular cartilage after experimental section of the anterior cruciate ligament of the dog knee. J Anat 1983;136:425–39.
37. Clark AL, Mills L, Hart DA, Herzog W. Muscle-induced patellofemoral joint loading rapidly affects cartilage mRNA levels in a site specific manner. J Muscoskel Res 2004;8:1–12.
38. Clark AL, Barclay LD, Matyas JR, Herzog W. In situ chondrocyte deformation with physiological compression of the feline patellofemoral joint. J Biomech 2003;36:553–68.
39. Korhonen RK, Han S-K, Herzog W. Osmotic loading of articular cartilage modulates cell deformations along primary collagen fibril directions. J Biomech 2010;43:783–7.
40. Korhonen RK, Han S-K, Herzog W. Osmotic loading of in situ chondrocytes in their native environment. Mol Cell Biomech 2009;10:1–10.
41. Alyassin AM, Lancaster JL, Downs JH, Fox PT. Evaluation of new algorithms for the interactive measurement of surface area and volume. Med Phys 1994;21:741–52.
42. Hayes WC, Keer LM, Herrmann G, Mockros LF. A mathematical analysis for indentation tests of articular cartilage. J Biomech 1972;5:541–51.
43. Korhonen RK, Laasanen MS, Töyräs J, Rieppo J, Hirvonen J, Helminen HJ, *et al*. Comparison of the equilibrium response of articular cartilage in unconfined compression, confined compression and indentation. J Biomech 2002;35:903–9.
44. Julkunen P, Korhonen RK, Herzog W, Jurvelin JS. Uncertainties in indentation testing of articular cartilage: a fibril-reinforced poroviscoelastic study. Med Eng Phys 2008;30:506–15.
45. Rieppo J, Hallikainen J, Jurvelin JS, Kiviranta I, Helminen HJ, Hyttinen MM. Practical considerations in the use of polarized light microscopy in the analysis of the collagen network in articular cartilage. Microsc Res Tech 2008;71:279–87.
46. Rieppo J, Hyttinen MM, Halmesmäki E, Ruotsalainen H, Vasara A, Kiviranta I, *et al*. Changes in spatial collagen content and collagen network architecture in porcine articular cartilage during growth and maturation. Osteoarthritis Cartilage 2009;17:448–55.
47. Király K, Hyttinen MM, Lapveteläinen T, Elo M, Kiviranta I, Dobai J, *et al*. Specimen preparation and quantification of collagen birefringence in unstained sections of articular cartilage using image analysis and polarizing light microscopy. J Mol Histol 1997;29:317–27.
48. Camacho NP, West P, Torzilli PA, Mendelsohn R. FTIR microscopic imaging of collagen and proteoglycan in bovine cartilage. Biopolymers 2001;62:1–8.
49. Bi X, Yang X, Bostrom MPG, Camacho NP. Fourier transform infrared imaging spectroscopy investigations in the pathogenesis and repair of cartilage. BBA Biomemb 2006;1758:934–41.
50. Boskey A, Camacho NP. FT-IR imaging of native and tissue-engineered bone and cartilage. Biomater 2007;28:2465–78.
51. Arokoski JPA, Hyttinen MM, Lapveteläinen T, Takacs P, Kosztaczky B, Módis L, *et al*. Decreased birefringence of the superficial zone collagen network in the canine knee (stifle) articular cartilage after long distance running training, detected by quantitative polarised light microscopy. Ann Rheum Dis 1996;55:253–64.
52. Bennett HS. Methods applicable to the study of both fresh and fixed materials. The microscopical investigation of biological materials with polarized light. In: McClung JR, Ed. McClung's Handbook of Microscopical Technique. New York: PB Hoeber; 1950:591–677.
53. Király K, Lapveteläinen T, Arokoski J, Törrönen K, Módis L, Kiviranta I, *et al*. Application of selected cationic dyes for the semiquantitative estimation of glycosaminoglycans in histological sections of articular cartilage by microspectrophotometry. Histochem J 1996;28:577–90.
54. Arokoski JPA, Jurvelin JS, Väätäinen U, Helminen HJ. Normal and pathological adaptations of articular cartilage to joint loading. Scand J Med Sci Sports 2000;10:186–98.
55. Panula HE, Hyttinen MM, Arokoski JPA, Långsjö TK, Pelttari A, Kiviranta I, *et al*. Articular cartilage superficial zone collagen birefringence reduced and cartilage thickness increased before surface fibrillation in experimental osteoarthritis. Ann Rheum Dis 1998;57:237–45.
56. Saarakkala S, Julkunen P, Mäkitalo J, Jurvelin JS, Korhonen RK. Depth-wise progression of osteoarthritis in human articular cartilage: investigation of composition, structure and biomechanics. Osteoarthritis Cartilage 2010;18:73–81.
57. Clarke IC. Articular cartilage: a review and scanning electron microscope study 1. The interterritorial fibrillar architecture. J Bone Joint Surg Br 1971;53:732–50.
58. Zambrano NZ, Montes GS, Shigihara KM, Sanchez EM, Junqueira LCU. Collagen arrangement in cartilages. Acta Anat 1982;113:26–38.
59. Benninghoff A. Form und Bau der Gelenkknorpel in Ihren Beziehungen zur Funktion. Cell Tissue Res 1925;2:783–862.

60. Gwynn IAP, Wade S, Kääb MJ, Owen GR, Richards RG. Freeze-substitution of rabbit tibial articular cartilage reveals that radial zone collagen fibres are tubules. J Microsc 2000;197:159–72.
61. Nötzli H, Clark J. Deformation of loaded articular cartilage prepared for scanning electron microscopy with rapid freezing and freeze-substitution fixation. J Orthop Res 1997;15:76–86.
62. Rivers PA, Rosenwasser MP, Mow VC, Pawluk RJ, Strauch MD, Sugalski MT, *et al*. Osteoarthritic changes in the biochemical composition of thumb carpometacarpal joint cartilage and correlation with biomechanical properties. J Hand Surg 2000;25:889–98.
63. Tanska P, Julkunen P, Korhonen RK. Collagen fibrils of articular cartilage modulate cell deformations in early osteoarthritis. (Abstract) Trans Orthop Res Soc 2011;36:2174.
64. Korhonen RK, Herzog W. Depth-dependent analysis of the role of collagen fibrils, fixed charges and fluid in the pericellular matrix of articular cartilage on chondrocyte mechanics. J Biomech 2008;41:480–5.
65. Broom ND, Myers DB. Fibrous waveforms or crimp in surface and subsurface layers of hyaline cartilage maintained in its wet functional condition. Connect Tissue Res 1980;7:165–75.
66. Guilak F, Alexopoulos LG, Upton ML, Youn I, Choi JB, Cao L, *et al*. The pericellular matrix as a transducer of biomechanical and biochemical signals in articular cartilage. Ann N Y Acad Sci 2006;1068:498–512.
67. Choi JB, Youn I, Cao L, Leddy HA, Gilchrist CL, Setton LA. Zonal changes in the three-dimensional morphology of the chondron under compression: the relationship among cellular, pericellular, and extracellular deformation in articular cartilage. J Biomech 2007;40:2596–603.
68. Kim E, Guilak F, Haider MA. The dynamic mechanical environment of the chondrocyte: a biphasic finite element model of cell–matrix interactions under cyclic compressive loading. J Biomech Eng Trans ASME 2008;130:061009.
69. Alexopoulos LG, Williams GM, Upton ML, Setton LA, Guilak F. Osteoarthritic changes in the biphasic mechanical properties of the chondrocyte pericellular matrix in articular. J Biomech 2005;38:509–17.
70. Alexopoulos LG, Setton LA, Guilak F. The biomechanical role of the chondrocyte pericellular matrix in articular cartilage. Acta Biomater 2005;1:317–25.
71. Korhonen RK, Julkunen P, Jurvelin JS, Saarakkala S. Structural and compositional changes in peri- and extracellular matrix of osteoarthritic cartilage modulate chondrocyte morphology. Cell Mol Bioeng 2011;4:484–94.
72. Korhonen RK, Julkunen P, Wilson W, Herzog W. Importance of collagen orientation and depth-dependent fixed charge densities of cartilage on mechanical behavior of chondrocytes. J Biomech Eng 2008;130:021003.
73. Mankin HJ, Dorfman H, Lippiello L, Zarins A. Biochemical and metabolic abnormalities in articular cartilage from osteoarthritic human hips II. Correlation of morphology with biochemical and metabolic data. J Bone Joint Surg Am 1971;53:523–37.
74. Pritzker KPH, Gay S, Jimenez SA, Ostergaard K, Pelletier J-P, Revell PA, *et al*. Osteoarthritis cartilage histopathology: grading and staging. Osteoarthritis Cartilage 2006;14:13–29.
75. Rieppo J, Töyräs J, Nieminen MT, Kovanen V, Hyttinen MM, Korhonen RK, *et al*. Structure–function relationships in enzymatically modified articular cartilage. Cells Tissues Organs 2003;175:121–32.
76. Hosseini A, Van de Velde SK, Kozanek M, Gill TJ, Grodzinsky AJ, Rubash HE, *et al*. In-vivo time-dependent articular cartilage contact behavior of the tibiofemoral joint. Osteoarthritis Cartilage 2010;18:909–16.
77. Schinagl RM, Gurskis D, Chen AC, Sah RL. Depth-dependent confined compression modulus of full-thickness bovine articular cartilage. J Orthop Res 1997;15:499–506.
78. Mäkitalo J, Saarakkala S, Rieppo L, Han S, Herzog W, Korhonen RK. Can collagen fibrillation or proteoglycan depletion of cartilage explain changed deformation behavior of chondrocytes 9 weeks after anterior cruciate ligament transection? (Abstract) Trans Orthop Res Soc 2011;36:2026.